Conf-950426--6

ANL/ET/CP--82776

IRRADIATION PERFORMANCE OF U-Pu-Zr METAL FUELS FOR LIQUID-METAL-COOLED REACTORS*

H. Tsai, A. B. Cohen, M. C. Billone, and L. A. Neimark

Energy Technology Division
Argonne National Laboratory-East
Argonne, IL 60439-4838 USA

October 1994

DISCLAIMER

Submitted to 3rd Intl. Conf. on Nuclear Engineering (ICONE-3). Sponsored by Japan Society of Mechanical Engineers and the American Society of Mechanical Engineers, Kyoto, Japan, April 23-27, 1995

*Work supported by the U.S. Department of Energy, Office of Technology Support Programs, under Contract W-31-109-Eng-38.

IRRADIATION PERFORMANCE OF U-Pu-Zr METAL FUELS FOR LIQUID METAL-COOLED REACTORS*

by

H. Tsai, A. B. Cohen, M. C. Billone, and L. A. Neimark

ABSTRACT

A fuel system utilizing metallic U-Pu-Zr alloys has been developed for advanced liquid metal-cooled reactors (LMRs). Results from extensive irradiation testing conducted in EBR-II show a design having the following key features can achieve both high reliability and high burnup capability: a cast nominally U-20wt.%Pu-10wt.%Zr slug with the diameter sized to yield a fuel smear density of ≈75% theoretical density, low-swelling tempered martensitic stainless steel cladding, sodium bond filling the initial fuel/cladding gap, and an as-built plenum/fuel volume ratio of ≈1.5. The robust performance capability of this design stems primarily from the negligible loading on the cladding from either fuel/cladding mechanical interaction or fission-gas pressure during the irradiation.

The effects of these individual design parameters, e.g., fuel smear density, zirconium content in fuel, plenum volume, and cladding types, on fuel element performance were investigated in a systematic irradiation experiment in EBR-II. The results show that, at the discharge burnup of ≈11 at.%, variations on zirconium content or plenum volume in the ranges tested have no substantial effects on performance. Fuel smear density, on the other hand, has pronounced but countervailing effects: increased density results in greater cladding strain, but lesser cladding wastage from fuel/cladding chemical interaction. The latter is apparently related to the reduced migration of lanthanide fission products to the fuel/cladding interface. The cladding type, whether martensitic or austenitic steels, has a noticeable impact on fuel/cladding chemical interaction.

INTRODUCTION

Metallic fuel consisting of a U-Pu-Zr alloy slug bonded with sodium in a stainless steel cladding has numerous advantages[1,2] for use in liquid-metal-cooled reactors (LMRs). The fuel system promises low fuel cycle costs because of the relatively simple process of initial fuel fabrication by casting and suitability for postirradiation pyroprocessing which produces material that can be readily cast into new fuel. Because of the high thermal conductivity, and hence a low latent heat at operating temperatures, the fuel possesses excellent passive safety characteristics. Whole-plant tests with EBR-II[3] under loss-of-flow-without-scram and loss-of-heat-sink-without-scram conditions amply demonstrated the potential for passive safety for the metal fuel system.

*Work supported by the U.S. Department of Energy, Office of Technology Support Programs, under Contract W-31-109-Eng-38.

Achieving high reliability, i.e., high burnup and low failure rates, was the principal goal of the metal fuels irradiation testing program. The current reference design, with a 10 wt.% Zr content in the U-Pu alloy fuel to provide high melting temperatures, a fuel smear density at 75% of the theoretical density (TD) to allow the fuel to swell and form interconnecting bubble networks to facilitate gas release, and a plenum volume ≈1.5 times that of the as-cast fuel to accommodate the released fission gas, has been shown to possess robust performance in extensive irradiation testing[4,5]. With this design, >19 at.% fuel burnup has been successfully attained in EBR-II. Equally excellent results were obtained with long-fuel-columns elements irradiated in the Fast Flux Test Facility (FFTF).[6,7]

To improve the understanding of the individual design parameters on overall fuel element performance, an irradiation experiment was conducted in EBR-II in which the parameters were systematically varied from the baseline reference case. The broadened data base would be useful for validating fuel element behavior codes, e.g., LIFE-Metal[8], and may also be used for future design optimization of the metal fuel systems.

This paper summarizes the results of this irradiation test.

EXPERIMENTAL DESIGN

The test, designated DP-1 (for design parameters), contained 61 elements in a wire-wrapped bundle. The fuel in all elements was a U-Pu-Zr alloy with a constant Pu content of 19 wt.%. All elements had an outer diameter of 5.84 mm and an overall length of 749.3 mm. The cladding thickness for all elements was 0.381 mm. As with other EBR-II metal fuel elements, the fuel slugs were produced by casting and bonded with sodium in the cladding. The fuel slugs had a nominal length of 342.9 mm, the core height of EBR-II, except those for a variable group discussed below.

The variables contained in the DP-1 test were:

- fuel smear density: 70, 75, and 85% TD, for its effect on fuel cladding mechanical interaction (FCMI) and fission gas release;
- zirconium content in fuel: 6, 10, and 14 wt.%, for its effects on fuel restructuring and fuel/cladding compatibility;
- plenum volume: plenum to fuel volume ratios (P/F) of 1.1, 1.5, and 2.1, for its effects on fission gas pressure loading on the cladding, and
- cladding types: tempered martensitic steel HT9 or austenitic stainless steel D9.

The elements in the test were categorized into ten groups. The control group had the following reference design attributes: U-19wt.%Pu-10wt.%Zr fuel, 75% TD fuel smear density, 1.5 P/F, and HT9 cladding. Only one parameter in

each of the variable groups was varied from that of the reference design to facilitate unobscured comparisons. The D9-clad element groups had only the Zr content as the variable to study the effects of Zr content on fuel/D9 compatibility.

As the overall length of the elements was fixed, elements with the high P/F was produced by reducing the fuel height, from the nominal 342.9 mm to 279.4 mm. For those elements with the low P/F, longer fuel element upper end plugs were used to eliminate part of the plenum volume. The variation on fuel smear density was achieved by loading fuel slugs cast with different diameters.

Operating conditions for the control and variable elements were kept as close as possible to facilitate direct comparisons. For elements with fuel smear density and Zr content variables, the ^{235}U enrichment was adjusted to yield approximately the same linear power at the beginning-of-life (BOL) of irradiation.

IRRADIATION HISTORY

The design goal burnup for the DP-1 test was 10 at.% and the actual irradiation reached ≈11.0 at.%. The irradiation consisted of two segments: the initial assembly to a peak burnup of ≈5.5 at.% (hereafter called the interim burnup) at which time eleven elements were removed for destructive examination and testing, and a reconstituted assembly to the final burnup.

The design BOL peak linear power and cladding temperature of the test elements were 49 kW/m and 600°C, respectively. These conditions were more aggressive than envisioned for LMR applications[9] and were chosen for the purpose of (1) accentuating any performance differences between the test element groups, and (2) enveloping the normal operating conditions of metal fuel elements in EBR-II. Actual peak element conditions at BOL, based on calculations, were 53 kW/m and 595°C. At the end of irradiation, these ratings decreased to 47 kW/m and 560°C due to fuel burnout.

FUEL PERFORMANCE

A. Cladding Endurance Limit

None of the elements in the DP-1 test breached during the irradiation. The discharge burnup of ≈11 at.% was dictated by an unrelated assembly hardware limitation and does not reflect the ultimate burnup capabilities of the test elements. The ability to attain high burnups under aggressive irradiation conditions, even for those elements with the high fuel smear density, attests to the excellent performance of the metal fuel elements.

B. Fuel Column Elongation

Early in life, i.e., within 1-2 at.% burnup from startup, a ternary U-Pu-Zr fuel slug invariably develops one or more wedge-shaped radial cracks from the internal thermal and mechanical stress loadings. With further irradiation, fuel swelling and restructuring closes the cracks and the as-built fuel/cladding gap initially filled with sodium. Before the fuel/cladding gap is closed, however, the fuel slug undergoes unrestrained growth in the axial direction.[10] Determination of this elongation is important because the elongation produces a negative reactivity insertion that has to be compensated for by the reactor control rods.

Fuel column lengths of the DP-1 elements were measured at both the interim and final burnups. The techniques used were ^{95}Zr-^{95}Nb scanning and neutron radiography. At the interim, the average fuel column elongation ($\Delta L/L$) for the control group was 1.8%, in good agreement with the previous data[5,11] for U-19Pu-10Zr fuels irradiated in EBR-II. In the variable groups, neither the Zr content nor the plenum volume had a noticeable effect on elongation. A slightly greater elongation (2.6%) was noted in the element group with the low smear-density (70% TD) fuel, apparently reflecting the delayed fuel/cladding lockup because of the undersized fuel slug.

There was no discernible additional fuel column growth between the interim and final burnups, an indication of the effectiveness of even limited fuel/cladding mechanical interaction in restraining fuel growth after the fuel/cladding contact.

Both axial gamma scanning and neutron radiographic data show the distribution of fissile materials along the fuel length to be uniform, except at the very top. In the top ≈5 mm of the elongated fuel column, the fissile content appeared to be lower than elsewhere, evidently because only the very top of the fuel column grew into the plenum.

C. Fission-Gas Release

Fission-gas release is a critical measure of metal fuel performance as it relates directly to fuel swelling and FCMI. In the reference metal fuel design with a fuel smear density of 75% TD, a network of interconnected gas bubbles develops in the fuel during irradiation and allows ≈70-80% of the fission gas to vent to the element plenum.[11] Such a release abates further fuel swelling and minimizes the mechanical loading on the cladding.

Selected DP-1 elements were punctured at the interim and final burnups to determine the fission gas release fractions. At the interim burnup, the release fractions were ≈80% for all the elements sampled, except for the high smear-density fuel, which showed a release of only 60%. The same release pattern is noted at the final burnup: 57% for the high density fuel and ≈75% for all other elements. The lower release is apparently the result of insufficient unrestrained fuel swelling to allow an interconnected network of gas

bubbles to form. From the standpoint of fission gas release, the similarity between the 70- and 75%-TD fuels shows no advantage of reducing the fuel density below the reference 75% TD.

The Zr content in the fuel, as will be shown later, affects fuel restructuring. But within the tested 6-14 wt.% range, it apparently had no discernible effects on fission gas release.

D. Cladding Strain

Cladding diameters for the DP-1 elements were measured with optical (laser) and contact profilometers at both the interim and final burnups. At the interim burnup, peak strains for all elements were small, ≈0.1%, except for the high-smear-density fuel, which was ≈0.3%. The greater strain in the high smear density element was apparently related to the reduced fission gas release, which resulted in greater fuel swelling forces and, consequently, enhanced FCMI.

At the final burnup, the peak strains for the control group remained small, only ≈0.3%. The strain profile of a control element is shown in Fig. 1. As the strain in the plenum region is minimal, the loading from the fission gas pressure is apparently negligible. Therefore, the limited strain of ≈0.3% is evidently caused by the modest FCMI that has developed by the final burnup. (The other possible cladding strain mechanism, namely cladding void swelling, is not operative with HT9 cladding at these conditions.) Further evidence indicating FCMI is the somewhat abrupt change of the strain magnitude at the top of the fuel column.

The mechanical performance of the variable groups vis-a-vis that of the reference design is summarized in Fig. 2. The results show that:

- The effect of plenum size on cladding strain is minimal, i.e., stress loading on the cladding from the fission gas in the plenum is insignificant in all elements at the final burnup.

- The variation of zirconium content in the fuel in the range of 6-14 wt.% has also essentially no effect on the cladding strain behavior.

- The strains in D9-clad elements are ≈0.5% greater than in the HT9-clad counterparts at the final burnup. This increment is apparently due to the void swelling in the D9 cladding at the discharge fluence ($\approx 1.0 \times 10^{23}$ n/cm^2/s, E>0.1 MeV).

- High fuel smear density has the single, most profound effect on cladding strain. Whereas the 70 and 75% TD fuels have approximately the same small strains (≈0.3%), the 85% TD fuel elements incur a group-average peak strain of ≈1.7%. The cause was apparently the enhanced FCMI because of the reduced fission gas release in the high density elements.

E. Fuel Microstructure

During irradiation, swelling of the U-Pu-Zr fuel closes the as-built fuel/cladding gap. With irradiation, a mature metal fuel microstructure with irradiation shows near-concentric fuel zones due to the migration of zirconium under temperature and chemical potential gradients. The zones, typically three principal ones, have different zirconium contents and pore morphology: the center is enriched in zirconium and contains larger pores, the intermediate zone is depleted in zirconium and low in porosity, and the outer zone contains intermediate-size fission gas bubbles and approximately the original content of zirconium. Slight redistribution of plutonium accompanies the zirconium and porosity redistribution. The lanthanide fission products generated during irradiation are insoluble in the fuel matrix, and agglomerate into a distinct phase. The lanthanide phases concentrate in the fuel center and, apparently through migration down the temperature gradient, also aggregate in the outer zone of the fuel. (While the mechanism for migration has not been satisfactorily determined, it appears certain that the lanthanides move through the pores in the fuel, via either vapor transport, surface diffusion, or seepage under gas pressure.) It has been shown that the lanthanide fission products near the fuel/cladding interface can substantially impact fuel/cladding compatibility[12]. A representative microstructure of a control element at the final burnup is shown in Fig. 3.

Fuel restructuring is only marginally affected by the zirconium content, as shown in Fig. 4 for fuels with 6 and 14 wt.% Zr. As the Zr content is varied, the sizes of the inner and middle zones change but the relative composition in each zone does not. (The size of the high-Zr central zone increases with the zirconium content while the thickness of the low-Zr middle zone decreases with the zirconium content.) The size of the outer zone is approximately the same for all three Zr-variable fuel types.

Fuel smear density has a pronounced effect on fuel restructuring. As shown in Fig. 5, compared to the 70% TD sibling, the 85% TD high density fuel displays a smaller porous center zone, a well-formed, dense intermediate band, and essentially no residual fuel/cladding interface. The latter is consistent with the observed higher cladding strains in the high density elements. The migration of lanthanide fission products down the temperature is apparently strongly influenced by the porosity in the fuel: the concentration of lanthanide phases in the outer region of the fuel is substantially lower in the 85% TD fuel than in the 70-75% TD fuels, as shown in Fig. 6.

F. Fuel/Cladding Chemical Interaction

Fuel/cladding chemical interaction (FCCI) during irradiation is a diffusional phenomena and is, therefore, affected by the composition, temperature, and time at temperature at the fuel/cladding interface. FCCI results in the diffusion of fuel constituents (including fission products) into the cladding, thereby reducing the effective thickness of the cladding by an amount commonly called "wastage." On the fuel side, the diffusion of cladding constituents

into the fuel could result in a lowering of the solidus temperature of the fuel.[12] No significant FCCI was noted in any of the test elements at the interim burnup, but discernible interaction was noted at the final burnup.

The diffusion structures formed in the DP-1 claddings from FCCI are dominated by the lanthanide fission products, especially cerium and neodymium, and plutonium. These constituents are found at the deepest penetration into the cladding. The typical FCCI structure in a HT9-clad element at the final burnup is shown in Fig. 7.

Among the variables studied in DP-1 test, only fuel smear density and cladding type are found to exert a significant effect on FCCI. Within the data scatter, the Zr content variation in the range of 6-14 wt.% appears to be inconsequential. These results are shown in Table 1.

Table 1. Measured Cladding Wastage As Affected by Fuel-Smear-Density Cladding Types and Zr Contents*

Fuel-smear Density (% TD)	Cladding Type	Zr Content	Cladding Wastage (μm)
70/75	HT9	10	40
85	HT9	10	22
75	D9	10	100
75	HT9	6	25
75	HT9	14	25

*All data from the same axial elevation of X/L = 0.78.

The effect of smear density can be understood by relating its role in the formation of the porosity network and the migration of fission products, in this case, the lanthanides. The high-smear density limits the amount of interconnected porosity in the fuel and the migration of fission products. Thus, the low-smear-density fuels, having greater interconnected porosity, have a higher lanthanide inventory at the fuel/cladding interface, and hence the higher cladding wastage. Conversely, the high-smear-density fuel does not have a good network of interconnected porosity and hence has the lower cladding wastage.

The lack of a strong FCCI dependency on Zr content was somewhat unexpected at the onset, owing to other data that suggest a protective nature of a ZrO_2 surface rind. The Zr variable fuels are very similar to each other, having nearly identical fuel microstructures (including porosity morphology). Clearly, FCCI is most strongly influenced by the concentration of lanthanide fission products at the fuel/cladding interface, rather than the bulk fuel composition or temporary and limited surface barriers.

The substantially higher cladding wastage in the D9-clad elements was due mainly to the constituent nickel in the D9 cladding. Nickel diffuses into the fuel more readily than the iron or chromium in the cladding. In out-of-pile diffusion tests[13,14] nickel has also been found to increase the diffusion of lanthanides, uranium, and presumably plutonium, into the cladding. The lower thermal conductivity of D9 than HT9 (and hence a higher fuel/cladding interface temperature, by ≈10°C) probably contributed to the higher wastage in the D9 cladding, although the effect is probably only secondary.

DISCUSSION

Possibly the most important result from the DP-1 test was finding the strong effects of fuel smear density on metallic fuel performance. This parameter impacts both FCMI (because it affects fuel swelling and fission-gas release) and FCCI (because it affects lanthanide migration). A reduction of smear density from the nominal value of 75 to 70% TD, which carries a neutronic penalty, apparently yielded no performance enhancement. On the other hand, a smear density of 85%, although improving fuel/cladding compatibility, aggravated FCMI. Judging from the trend lines established from these three data points, it appears likely that a fuel smear density somewhere between 75 and 85% TD could yield the optimal fuel element performance. A follow-up experiment to explore this range of density should prove to be fruitful.

The discharge burnup of 11 at.% does not permit a full study on the effects of plenum pressure, or plenum/fuel volume ratio. If the goal burnup in power reactor application is approximately that of the DP-1 discharge burnup, it appears feasible to reduce the element P/F from the reference 1.5 to 1.1 without a sacrifice of steady-state performance. Such a reduction of plenum volume translates into a reduction of fuel element length and core height and has strong economical incentives. For higher burnup applications, and for transient considerations, determining the optimal P/F remains an issue.

HT9 is clearly a superior cladding over D9 from the standpoint of fuel/cladding compatibility. At the cladding irradiation temperature of ≈600°C, HT9 exhibited only minor cladding wastage from FCCI. Such wastage should not degrade the cladding performance even during operational transients. However, if the design service temperature is substantially higher, even HT9 may not be satisfactory. An experiment conducted in EBR-II at ≈660°C cladding temperature showed excessive cladding degradation from lanthanide attack[15]. A cladding liner, made of a materials resistant to fuel/cladding constituent interdiffusion, such as vanadium or zirconium, may be the solution.

CONCLUSIONS

Metallic fuel elements with the reference design proved to have excellent performance during irradiation. At the discharge burnup of ≈11 at.%, these elements incurred minimal cladding strain and only minor cladding wastage from FCCI. Variations on the fuel zirconium content or plenum volume in the element showed no substantial effects on performance under the conditions tested.

Fuel smear density, on the other hand, has pronounced but countervailing effects: increased density results in greater cladding strain, but lesser cladding wastage from FCCI. The latter is apparently related to the reduced migration of lanthanide fission products to the fuel/cladding interface. The optimal fuel smear density for balanced FCMI and FCCI performance probably lies somewhere between 75 and 85% TD. Under the conditions tests, HT9 was clearly the superior cladding over D9 because of the more benign cladding wastage from FCCI.

ACKNOWLEDGMENTS

The authors thank the competent staff at the following ANL organizations for making this experiment possible: Experimental Fuels Laboratory for building the fuel elements, Hot Fuel Examination Facility for the postirradiation nondestructive examinations, and Alpha-Gamma Hot Cell Facility for the destructive examinations. Thanks are also extended to L. C. Walters for the support and encouragement during the project and A. M. Yacout for calculating the operating conditions of the fuel elements.

REFERENCES

1. Till, C. E. and Chang, Y. I., "Progress and Status of the Integral Fast Reactor (IFR); Fuel Cycle Development," Proc. of Intl. Conf. on Fast Reactor and Related Fuel Cycles, p. 1.6, Kyoto, Japan, Oct. 28-Nov. 1, 1991.

2. Till, C. E., "Fast Reactor Directions: The LMR Integral Fast Reactor Program at Argonne," Proc. of Intl. Fast Reactor Safety Meeting, IV, p. 449, Snowbird, UT, Aug. 12-16, 1990.

3. Fistedis, S. H. ed., "The Experimental Breeder Reactor-II Inherent Safety Demonstration," Nucl. Eng. Des., **101** (1987).

4. Leggett, R. D., and Walters, L. C., "Status of LMR Fuel Development in the United States of America," J. Nucl. Mat., **204**, 23-32 (1993).

5. Pahl, R., et al. "Steady-state Irradiation Testing of U-Pu-Zr Fuel to >18 at.% Burnup," Proc. of Intl Fast Reactor Safety Meeting, IV, p. 129, Snowbird, UT, Aug. 12-16, 1990.

6. Tsai, H., and Neimark, L. A., "Irradiation Performance of Full-Length Metallic IFR Fuels," Proc. of Intl. Conf. on Design and Safety of Advanced Nuclear Power Plants, III, p. 28.2-1, Tokyo, Japan, Oct. 25-29, 1992.

7. Pitner, A. L. and Baker, R. B., "Metal Fuels Test Program in the FFTF," J. Nucl. Mat., **204**, 124-130 (1993).

8. Billone, M. C., et al., "Status of Fuel Element Modeling Codes for Metallic Fuels," Proc. ANS Intl Conf. on Reliable Fuels for LMRs, pp. 5-77, Tucson, AZ, Sept. 7-11, 1986.

9. Berglund, R. C., et al., "Performance and Safety Design of the Advanced Liquid Metal Reactor," Proc. of Intl. Conf. on Fast Reactor and Related Fuel Cycles, p. 11.1, Kyoto, Japan, Oct. 28-Nov. 1, 1991.

10. Hofman, G. L., et al., "Swelling Behavior of U-Pu-Zr Fuel," Metal. Trans., 21A, 517-528 (March 1990).

11. Pahl, R. G. et al., "Irradiation Experience with HT9-clad Metallic Fuel," Proc. of Intl. Conf. on Fast Reactor and Related Fuel Cycles, p. P1.19, Kyoto, Japan, Oct. 28-Nov. 1, 1991.

12. Cohen, A. B., et al., "Fuel/Cladding Compatibility in U-19Pu-10Zr/HT9-clad Fuel at Elevated Temperatures," J. Nucl. Mat., 204, 244-251 (1993).

13. Tortorici, P. C. and Dayananda, M. A., "Interdiffusion of Cerium in Fe-based Alloys with Ni or Cr," J. Nucl. Mat., 204, 165-172 (1993).

14. Keiser D. D. and Dayananda, M. A., "Interdiffusion Between U-Zr fuel and Selected Fe-Ni-Cr Alloys," J. Nucl. Mat., 200, 229-243 (1993).

15. Pahl, R. G. et al., "Irradiation of HT9-clad Metallic Fuel at High Temperature," J. Nucl. Mat., 204, 141-147 (1993).

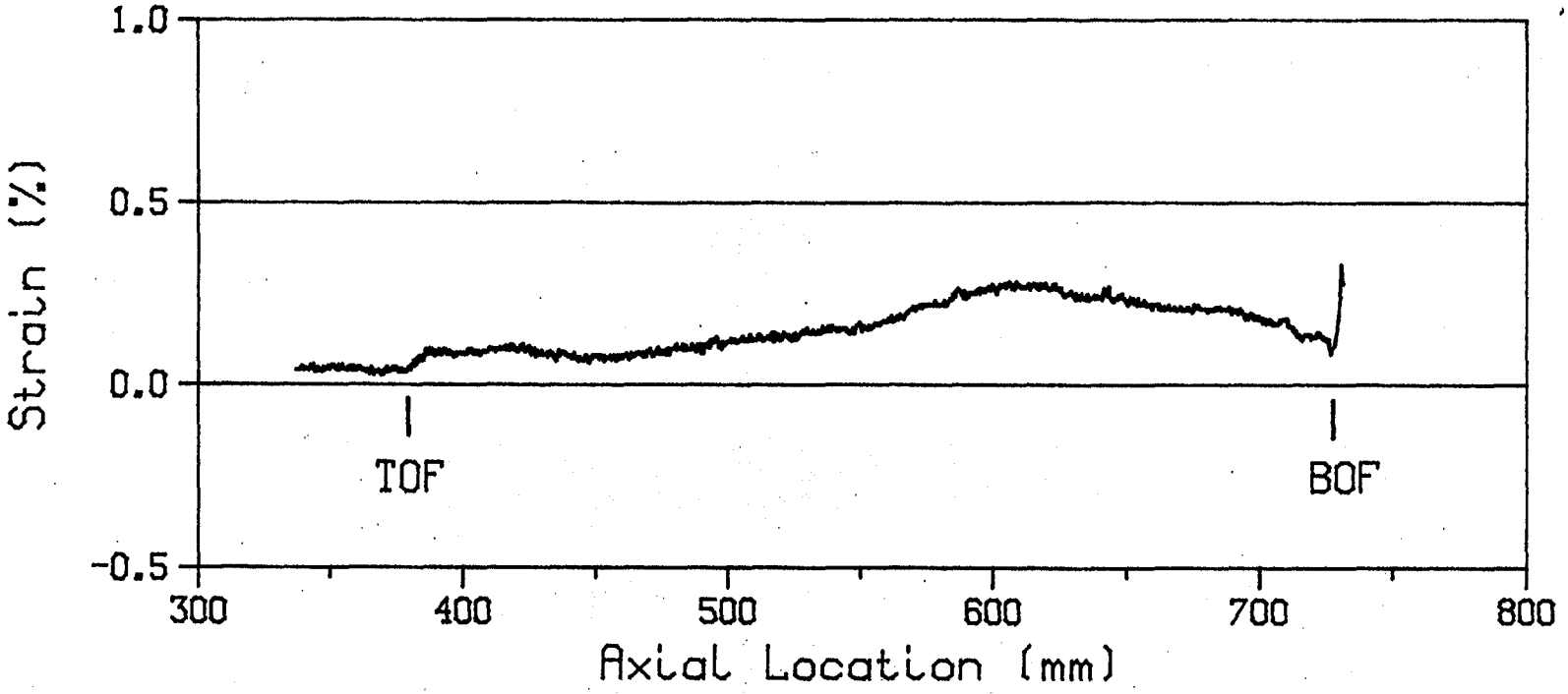

Fig. 1. Cladding strain profile of a control element (DP-21) at the final burnup. TOF and BOF denote top-of-fuel and bottom-of-fuel, respectively.

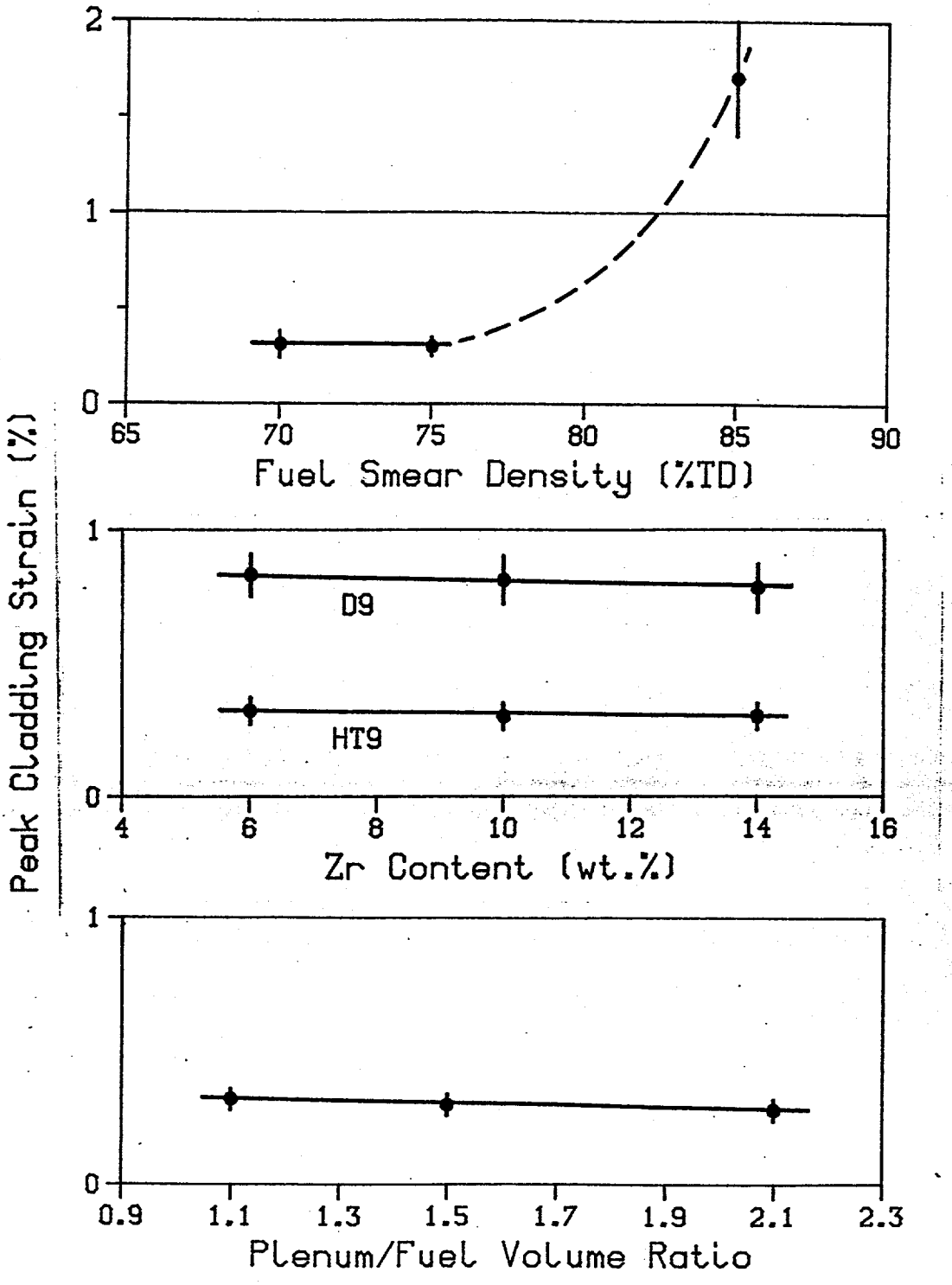

Fig. 2 Dependence of peak cladding strains on the test variables in the DP-1 test.

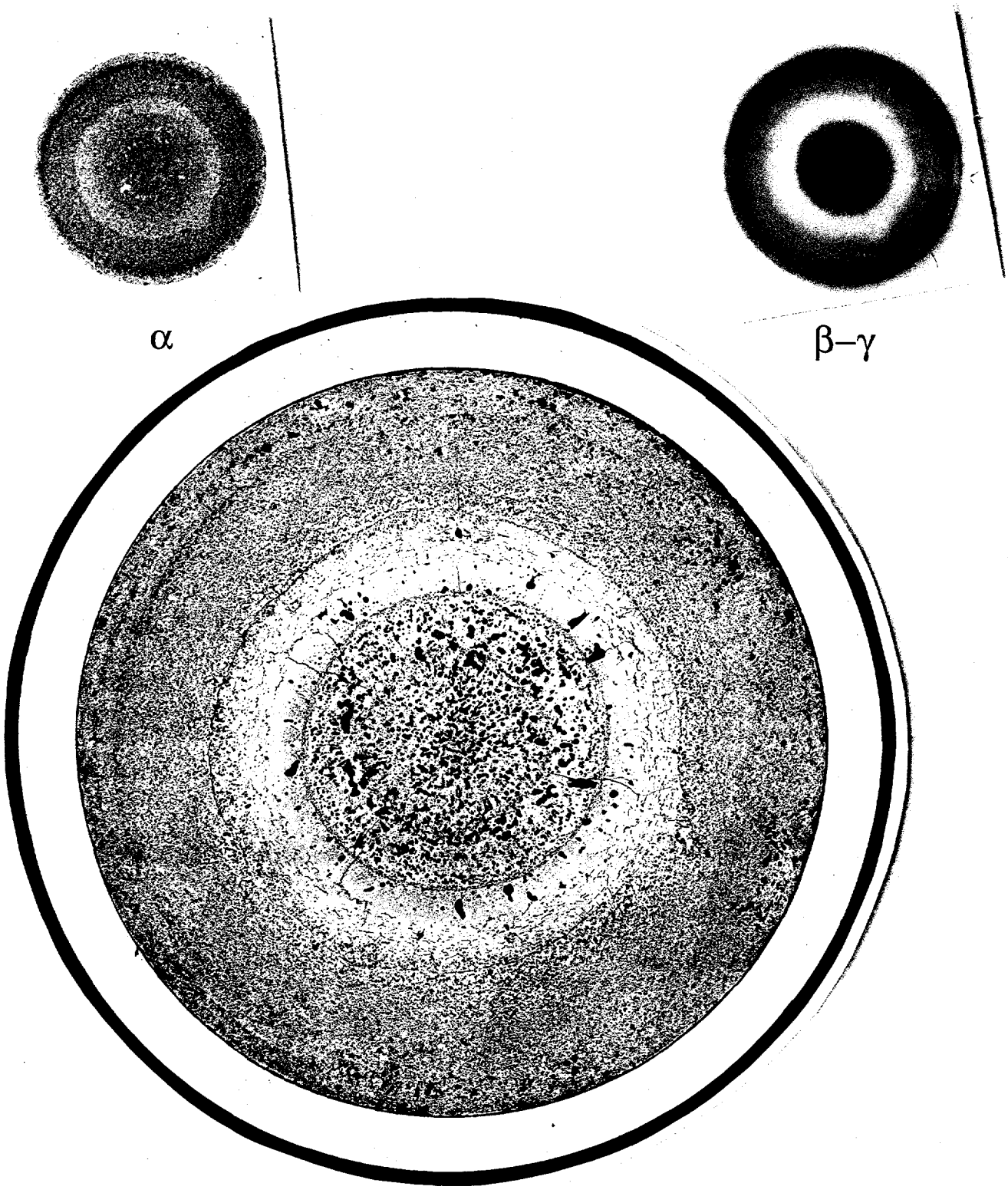

Fig. 3 Transverse section at the axial midplane of a control element (DP-21) at the final burnup. Note the formation of three concentric fuel zoned and the redistributions of Pu and fission products shown in the α and β-γ autoradiographs. The remnant of the early-in-life wedge-shaped fuel crack, which is essentially fully healed, can be seen at approximately the 4-o'clock orientation. (ET 278970, 279272, 279273)

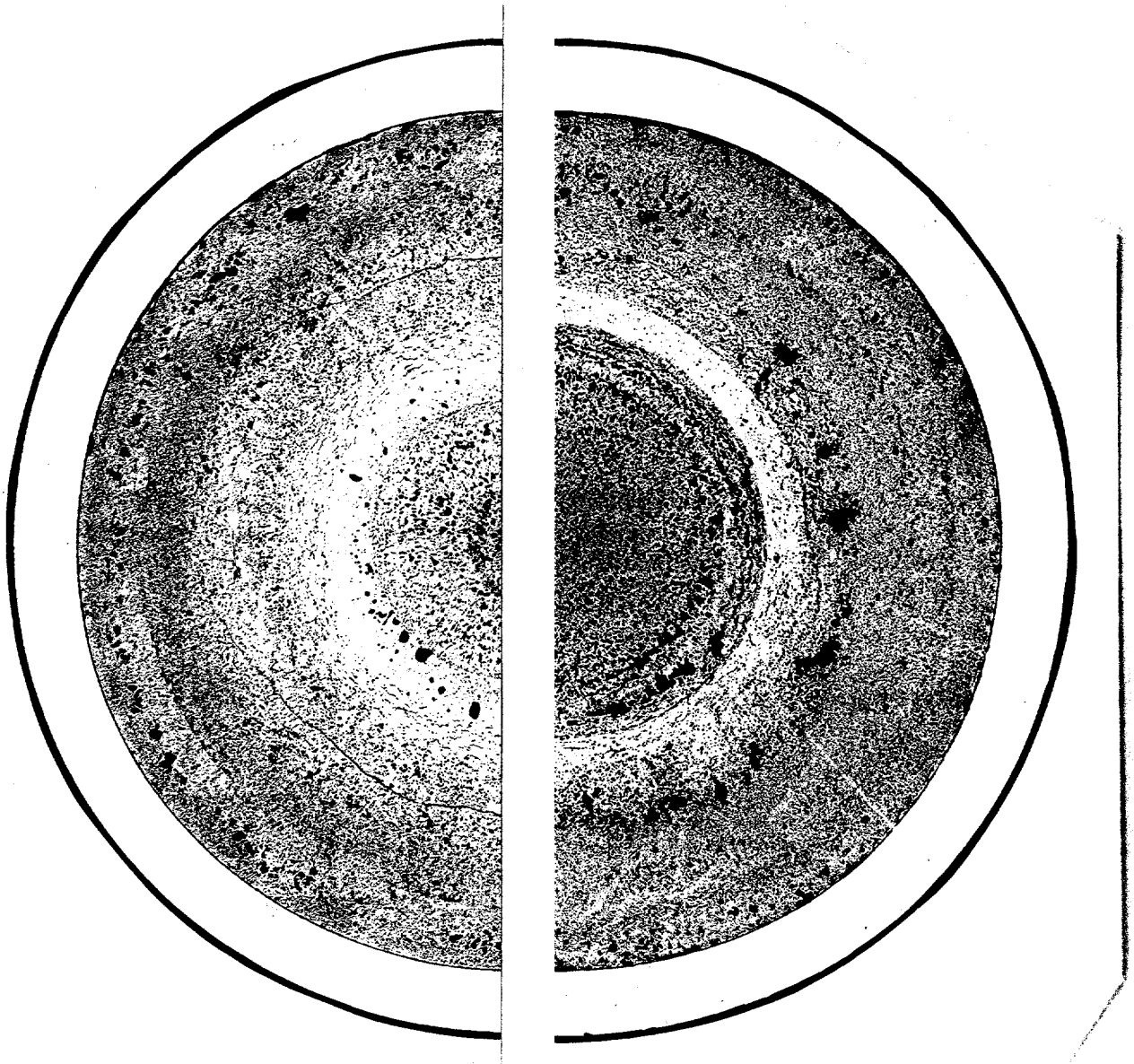

6 wt.% Zr

14 wt.% Zr

Fig. 4 Comparison of microstructure of fuels with 6-wt.% and 14-wt.% Zr contents at the final burnups. (ET 278971, 278969)

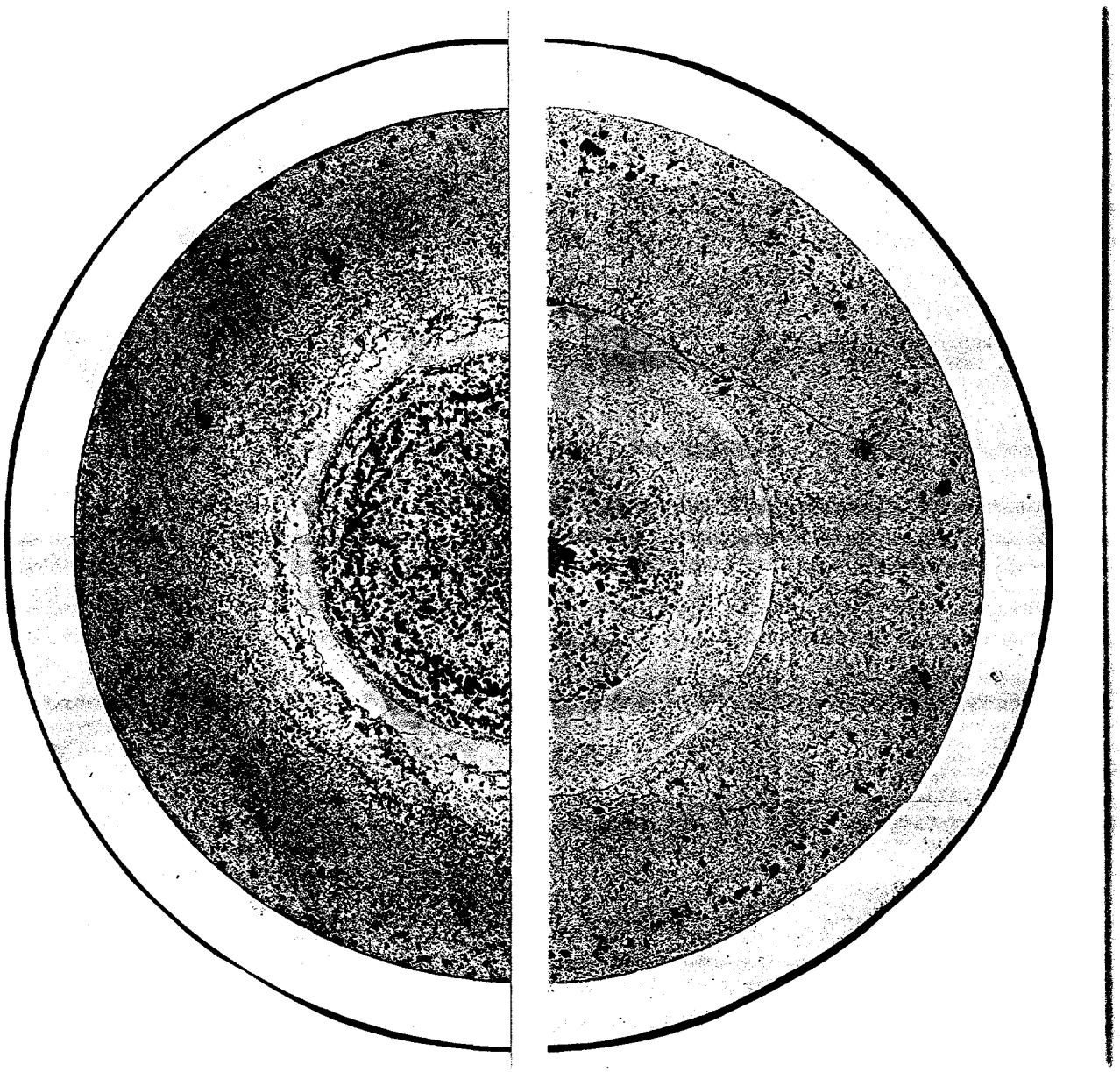

70% TD

85% TD

Fig. 5 Comparison of microstructure of fuels with 85% and 70% TD smear densities at the final burnups. (ET 278972, 278966)

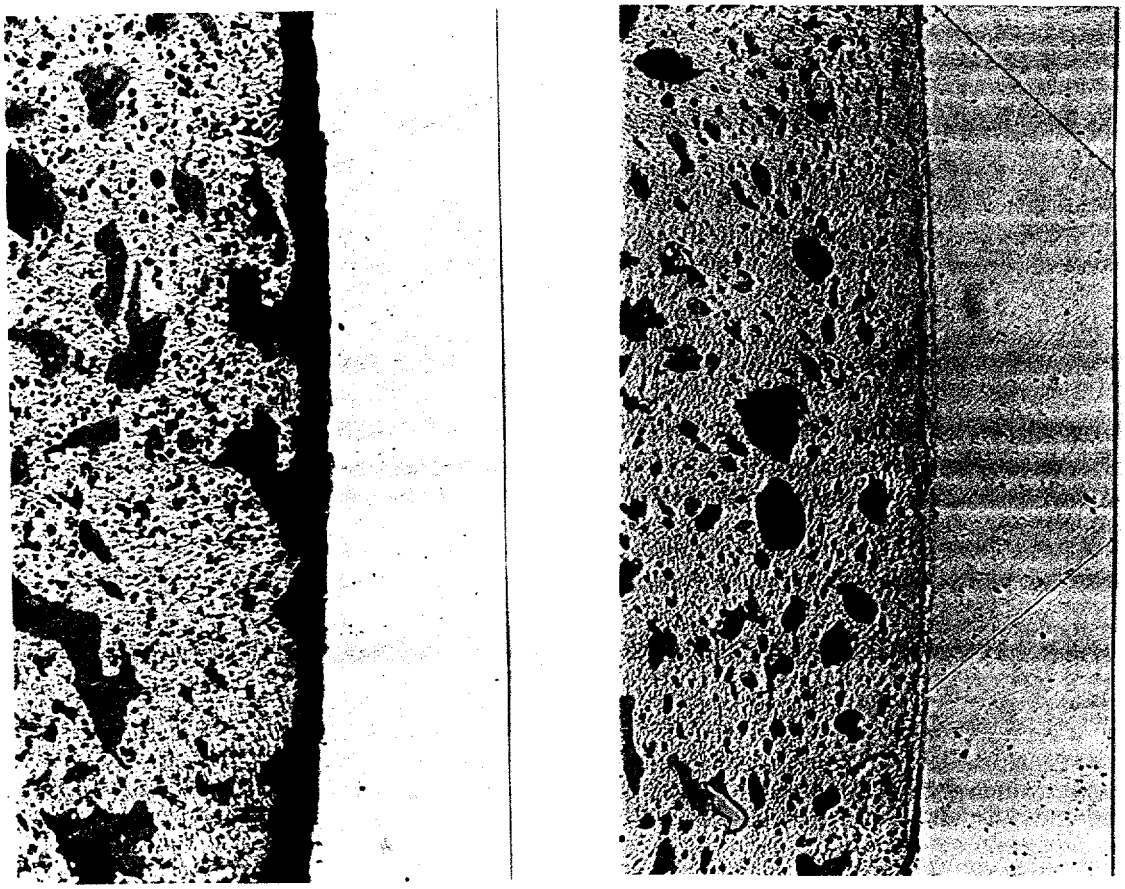

70% TD 85% TD

Fig. 6 Effect of fuel smear density on microstructure at the fuel/cladding interface. Note the greater inventory of lanthanide fission product ingots (gray phase) and the open fuel/cladding gaps in the 70% TD fuel. (ET 278952, 278874)

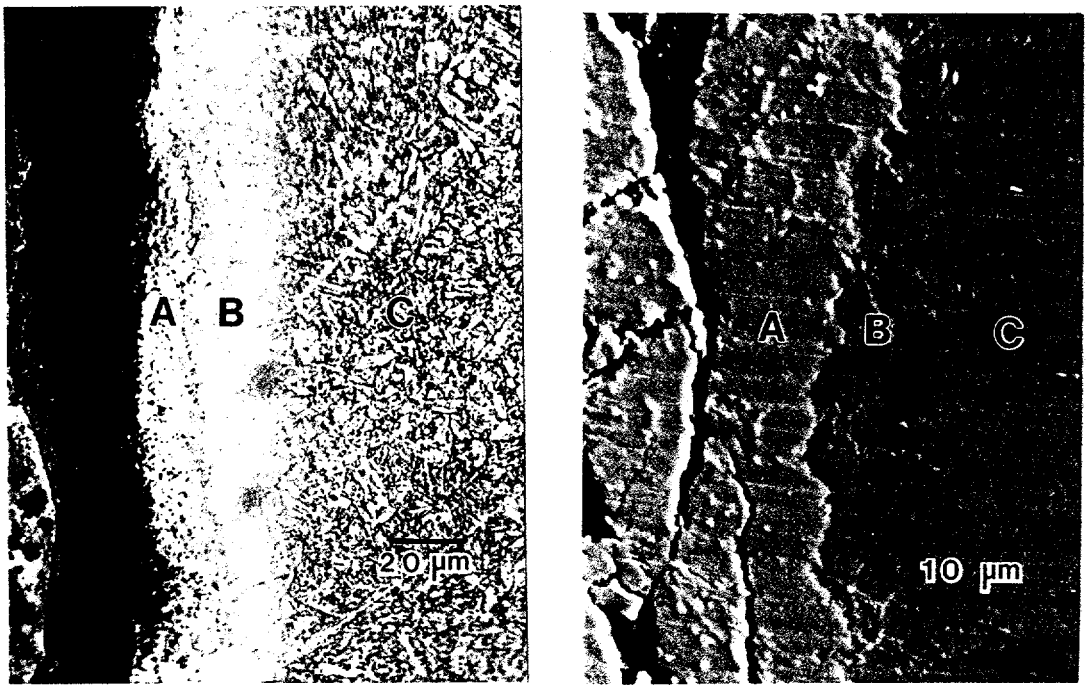

Optical SEM

Fig. 7 Fuel/cladding chemical interaction in a HT9-clad control element (DP-21, X/L = 0.89) at the final burnup. The interaction band A is enriched in lanthanide fission products and Pu; band B is decarburized and contains a precipitated lanthanide phase; location C is the unaffected HT9 cladding. (MCT 279270, etched; MCT 318639 SEM)